Striking Generic Impact of Light-Induced Non-Adiabaticity in Polyatomic Molecules

Csaba Fábri, Benjamin Lasorne, Gabor J. Halasz, Lorenz Cederbaum, Ágnes Vibók

Striking Generic Impact of Light-Induced Non-Adiabaticity in Polyatomic Molecules

Csaba Fábri,[*,†,‡] Benjamin Lasorne,[¶] Gábor J. Halász,[§] Lorenz S. Cederbaum,[‖] and Ágnes Vibók[*,⊥,#]

†*Laboratory of Molecular Structure and Dynamics, Institute of Chemistry, Eötvös Loránd University, Pázmány Péter sétány 1/A, H-1117 Budapest, Hungary*

‡*MTA-ELTE Complex Chemical Systems Research Group, P.O. Box 32, H-1518 Budapest 112, Hungary*

¶*Institut Charles Gerhardt Montpellier (ICGM), Université de Montpellier, CNRS, ENSCM, F-34095 Montpellier, France*

§*Department of Information Technology, University of Debrecen, P.O. Box 400, H-4002 Debrecen, Hungary*

‖*Theoretische Chemie, Physikalisch-Chemisches Institut, Universität Heidelberg, Im Neuenheimer Feld 229, 69120 Heidelberg, Germany*

⊥*Department of Theoretical Physics, University of Debrecen, PO Box 400, H-4002 Debrecen, Hungary*

#*ELI-ALPS, ELI-HU Non-Profit Ltd, H-6720 Szeged, Dugonics tér 13, Hungary*

E-mail: ficsaba@caesar.elte.hu; vibok@phys.unideb.hu

Abstract

Nonadiabaticity, i.e., the effect of mixing electronic states by nuclear motion, is a central phenomenon in molecular science. The strongest nonadiabatic effects arise due to the presence of conical intersections of electronic energy surfaces. These intersections are abundant in polyatomic molecules. Laser light can induce in a controlled manner new conical intersections, called light-induced conical intersections, which lead to strong nonadiabatic effects similar to those of the natural conical intersections. These effects are, however, controllable and may even compete with those of the natural intersections. In this work we show that the standard low-energy vibrational spectrum of the electronic ground state can change dramatically by inducing nonadiabaticity via a light-induced conical intersection. This generic effect is demonstrated for an explicit example by full-dimensional high-level quantum calculations using a pump-probe scheme with a moderate-intensity pump laser and a weak probe laser.

Graphical TOC Entry

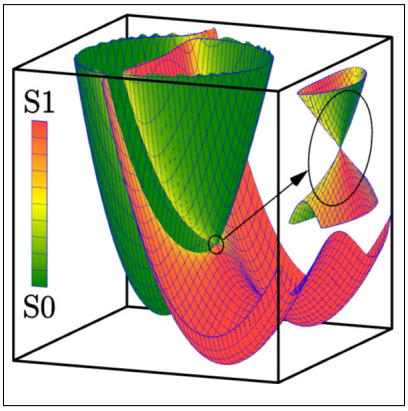

Keywords

Light-induced conical intersection, Vibrational spectrum, Pump-probe scheme, Intensity-borrowing effect

Nonadiabatic phenomena[1–6] occurring in polyatomic molecules have been known for decades to play a fundamental role in most photobiological, photochemical, and photophysical processes.[7–21] Such effects become significant around molecular geometries where two (or more) potential energy surfaces (PESs) are energetically degenerate, such that the Born–Oppenheimer (BO) approximation[22] breaks down. This yields strong mixing among BO electronic states and subsequent radiationless transitions correlated with variations of the molecular geometry (nuclear degrees of freedom).

Such degeneracy points, termed conical intersections (CIs), are characterized locally by a two-dimensional subspace within the space spanned by the nuclear degrees of freedom, the so-called "branching" space along which the degeneracy is lifted to first order around the CI. This can occur only in molecules with more than two atoms (Wigner's noncrossing rule).[23] Indeed, diatomic molecules have a single vibrational coordinate, which cannot accommodate both zero energy-difference tuning and zero coupling except for symmetry reasons. CIs provide ultrafast nonradiative decay channels for electronically excited molecules.[24,25] In the vicinity of such points, nonadiabatic dynamics (beyond BO) takes place typically on the femtosecond time scale ($\sim$10–100 fs). While it is by now well established that they are present in small- or medium-sized molecules, CIs have been shown to be ubiquitous in large molecular systems, hence playing a key role in most photoinduced processes. CIs can also influence the ground-state spectroscopic and dynamical properties of molecules.[26,27]

More than a decade ago, it has been demonstrated that laser light with significant intensity (dressed-state regime) can in turn induce CI-type situations between field-dressed PESs and thus give rise to new types of nonadiabatic phenomena, even in diatomic molecules.[28,29] Such points were then termed light-induced conical intersections (LICIs). Whereas the location of a "natural" CI in a field-free polyatomic molecule and the strength of the nonadiabatic coupling are inherent properties of the system, the occurrence of the LICI is determined by the laser frequency while the strength of the nonadiabatic-type coupling is controlled by the laser intensity.

Several theoretical and experimental works have demonstrated on both fronts that LICIs give rise to a variety of unexpected nonadiabatic phenomena in molecules,[30–34] with significant impact on various dynamical[35–38] and spectroscopic properties.[39–42] These works were mainly focused on diatomic molecules where the angle between the internuclear axis and the field polarization axis provides the missing degree of freedom for a CI to emerge between two crossing field-dressed PESs. This rotation angle together with the internuclear separation span the two-dimensional light-induced branching space along which degeneracy is lifted to first order around the LICI due to the dressing field.

Investigating light-induced nonadiabatic effects in polyatomic molecules is expected to be more challenging and richer than in diatomics. On the one hand, the existence of several vibrational degrees of freedom enables LICIs to be defined without further involving any rotational coordinate. On the other hand, natural CIs are ubiquitous in polyatomics that their occurrence and accompanying natural nonadiabatic effects are likely to be strongly mixed with the light-induced ones. It is thus desirable to first consider situations where a clear separation and identification of the effects of natural and light-induced conical intersections can be made, so as to clarify and understand the effect solely caused by the LICI.

Experimental works[43,44] have already invoked the concept of a LICI to provide qualitative interpretation to the results of laser-induced isomerization and photodissociation in polyatomic molecules. A general theory on LICIs discusses strategies of its exploitation and application in polyatomic systems.[45] Although ref. 45 provides a detailed discussion of the possible LICI strategies in polyatomics, no actual results which are based on accurate multidimensional quantum calculations and clearly demonstrate light-induced nonadiabatic effects have been published since then. The present study goes beyond previous investigations and makes an attempt to identify the impact of non-adiabaticity of LICIs in polyatomic molecules by employing accurate multidimensional quantum-dynamical methods instead of simple model calculations.

It is well established in the field of "natural" nonadiabatic molecular phenomena that

the breakdown of the BO approximation induces strong mixing between the vibrational levels within coupled adiabatic PESs. The Franck–Condon approximation is no longer valid, which typically leads at low energies to the so-called "intensity borrowing" effect.[1] This is a characteristic fingerprint of nonadiabatic effects in molecular spectroscopy, manifested by irregular variations of spectral peak intensities and the appearance of unexpected levels.

Along this line, our current work presents strong intensity-borrowing effects, now appearing in the field-dressed low-energy vibronic spectrum of the H_2CO (formaldehyde) molecule and absent in the absence of the field, providing direct proof of strong light-induced nonadiabatic effects. The photochemistry of H_2CO has been studied in various contexts and the corresponding literature is abundant and beyond the scope of the present work. We chose H_2CO for two reasons: first, because there is no natural CI in the vicinity of the Franck–Condon region. A seam of CIs has been characterized for example by Araujo et al.[46–48] but it is protected by a transition barrier at low energies; second, this system presents the great advantage of not having any first-order nonadiabatic coupling between the ground and first singlet excited electronic states around its equilibrium geometry. As a consequence, such a situation allows unambiguous identification of light-induced nonadiabatic phenomena, clearly separated from other "natural" nonadiabatic effects.

By using a two-step protocol we simulate the weak-field absorption and stimulated emission spectra of the *field-dressed* H_2CO molecule at low energy (infrared domain) taking into account all six vibrational degrees of freedom explicitly. First, we compute the field-dressed states which are superpositions of field-free molecular eigenstates coupled by a medium-intensity laser dressing pump pulse switched on adiabatically. Second, we assume that the low-energy spectrum of the field-dressed molecule can be accessed with a weak-intensity steady-state probe. The dipole transition amplitudes between the field-dressed states are thus evaluated within the typical framework of first-order time-dependent perturbation theory, revealing intensity borrowing in the infrared domain for the field-dressed molecule.

Let us start with presenting the field-free vibrational spectrum of H_2CO (see the Sup-

porting Information for the structure and normal modes of H_2CO) in its electronic ground state X, shown in the upper panel of Figure 1. As expected, the field-free vibrational spectrum consists of a moderate number of peaks, corresponding to vibrational transitions from the initially populated vibrational ground state to vibrationally-excited eigenstates. Besides the six fundamental transitions (denoted with the normal mode labels ν_i, described in Table S1 of the Supporting Information) two combination transitions ($\nu_2 + \nu_6$ and $\nu_3 + \nu_6$) and an overtone transition ($2\nu_2$) carry appreciable intensity. It is clearly visible in Figure 1 that no peaks appear below 1100 cm^{-1} in the field-free vibrational spectrum. However, if the molecule is dressed with a laser field switched on adiabatically and then the spectrum of the field-dressed molecule is measured with a weak probe pulse, striking effects arise in the field-dressed spectrum. The lower panel of Figure 1 shows the spectrum of H_2CO molecule dressed with a laser field linearly polarized along the body-fixed y axis (defined in the Supporting Information) with the dressing intensity of $I_\mathrm{d} = 10^{11}$ W/cm^2 and dressing wavenumber of $\omega_\mathrm{d} = 32932.5$ cm^{-1} (wavelength $\lambda_\mathrm{d} = 303.65$ nm). The field-dressed spectrum in Figure 1, as opposed to the field-free vibrational spectrum, shows the emergence of prominent peaks below 1100 cm^{-1}. At the same time the intensity of the major peaks seen in the field-free spectrum are substantially lowered. They seem to have borrowed their original intensity to the light-induced peaks below 1100 cm^{-1}.

In order to understand the origin of the differences between the field-free and field-dressed spectra in Figure 1 a brief description of the underlying theory is necessary. Throughout the current work the two singlet electronic states S_0 ($\tilde{X}\ ^1A_1$) and S_1 ($\tilde{A}\ ^1A_2$) of H_2CO are taken into account, the corresponding six-dimensional PESs are denoted by V_X and V_A, respectively. We assume that the electronic states X and A are coupled by a time-dependent external electric field $\mathbf{E}(t) = \mathbf{E}_0 \cos(\omega t)$. In the static Floquet-state representation[49,50] the

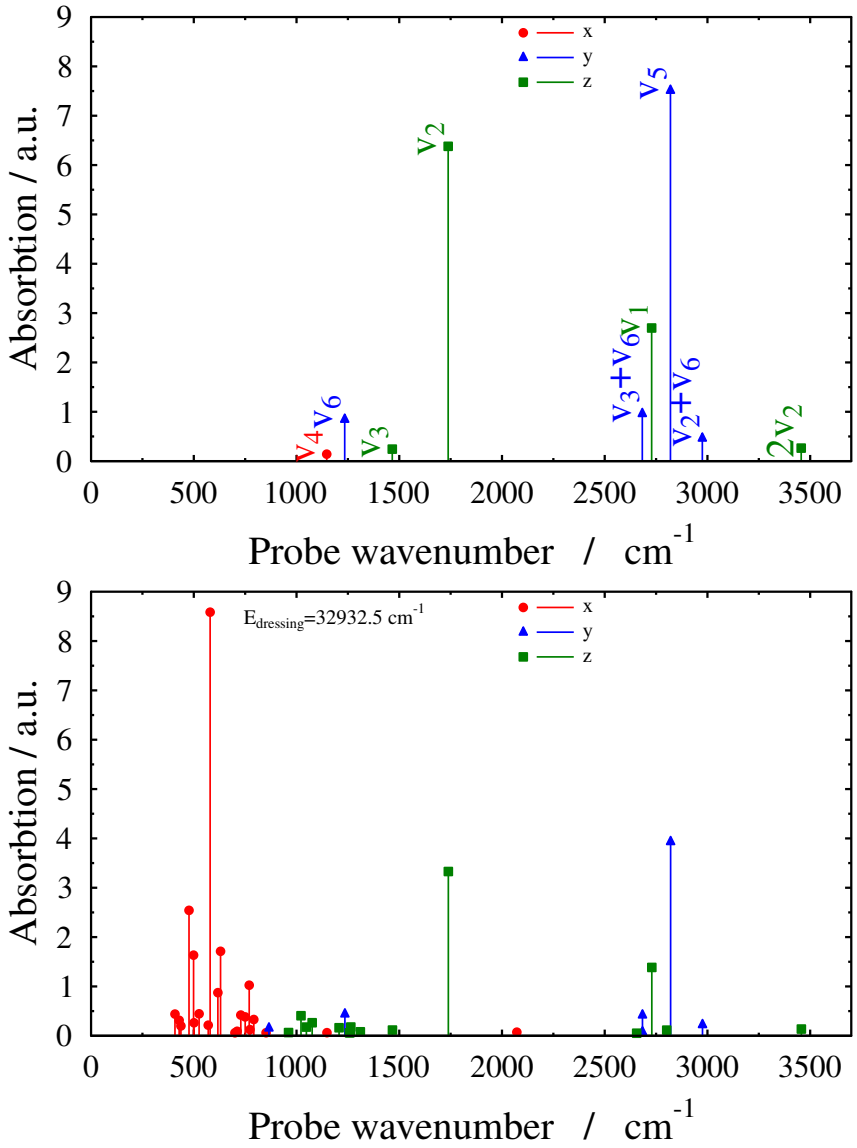

Figure 1: Impact of light-induced non-adiabaticity on the vibrational spectrum of H_2CO. Upper panel: field-free vibrational spectrum of the H_2CO molecule in its electronic ground state (X) with peaks corresponding to transitions from the vibrational ground state to vibrationally-excited eigenstates as indicated by the normal mode labels. Lower panel: spectrum of H_2CO dressed with a laser field linearly polarized along the body-fixed y axis with $I_\mathrm{d} = 10^{11}$ W/cm^2 and $\omega_\mathrm{d} = 32932.5$ cm^{-1}. Transitions polarized along the x, y and z axes are shown by the markers •, ▲ and ■, respectively. In sharp contrast to the field-free spectrum, the field-dressed spectrum exhibits a rich appearance of numerous peaks below 1100 cm^{-1}. Note the substantial lowering of the intensity due to the field of the peaks present in the field-free spectrum (the intensity scale is the same in both panels).

Hamiltonian matrix has the following form

$$\hat{H} = \begin{bmatrix} \hat{T} & 0 \\ 0 & \hat{T} \end{bmatrix} + \begin{bmatrix} V_{\mathrm{X}} + n\hbar\omega & W \\ W & V_{\mathrm{A}} + (n-1)\hbar\omega \end{bmatrix} \tag{1}$$

where $\hat{T}$ is the vibrational kinetic energy operator and n is the Fourier index that labels the different light-induced potential channels. The kinetic energy operator is fully exact, properly includes the exchange symmetry of the identical nuclei and it is constructed using a general numerical procedure described in refs. 51 and 52. The operator $W = -\mathbf{d}(\mathbf{R})\mathbf{e}E_0/2$ describes the coupling between the electronic states X and A with $\mathbf{d}(\mathbf{R})$ being the body-fixed molecular transition dipole moment (TDM) vector depending on the vibrational coordinates $\mathbf{R}$. Moreover, $\mathbf{e}$, E_0 and ω denote the polarization, amplitude and angular frequency of the dressing laser field, respectively. The permanent dipole moments (PDMs) of the X and A electronic states are included in the full calculations, but for simplicity not shown explicitly in eq 1. We used linearly-polarized electric fields throughout this work. The rotational degrees of freedom were omitted from our computational protocol and the orientation of the molecule was fixed with respect to the external electric field. After diagonalizing the potential energy matrix of eq 1 one can obtain the adiabatic potential energy surfaces V_{lower} and V_{upper}. These two PESs can cross each other, giving rise to a LICI, whenever the conditions $W = 0$ and $V_{\mathrm{X}} = V_{\mathrm{A}} - \hbar\omega$ are simultaneously fulfilled.

The field-dressed eigenfunctions $|\Phi_k(n)\rangle$ and quasienergies $\epsilon_k(n)$ can be obtained by determining the eigenpairs of the Hamiltonian of eq 1. The eigenfunctions $|\Phi_k(n)\rangle$ can be expanded as the linear combination of products of field-free molecular vibronic eigenstates (denoted by $|\mathrm{X}i\rangle$ and $|\mathrm{A}i\rangle$ for the electronic states X and A, respectively) and the Fourier vectors of the Floquet states, that is

$$|\Phi_k(n)\rangle = \sum_i C^{(k)}_{\mathrm{X}i} |\mathrm{X}i\rangle|n\rangle + \sum_i C^{(k)}_{\mathrm{A}i} |\mathrm{A}i\rangle|n-1\rangle. \tag{2}$$

In eq 2 i labels vibrational eigenstates and $|n\rangle$ is the nth Fourier vector of the Floquet state. The expansion coefficients $C_{\mathrm{X}i}^{(k)}$ and $C_{\mathrm{A}i}^{(k)}$ can be obtained by diagonalizing the light-dressed Hamiltonian of eq 1 after constructing its matrix representation. In this work the field-free molecular eigenstates of H_2CO were computed with the GENIUSH program package[51–53] treating all six vibrational degrees of freedom in a numerically exact way. The V_{X} and V_{A} PESs were taken from refs. 54 and 55, respectively. We note that the C_{2v} point group can be used to label the eigenstates of the field-free molecule and the symmetries of the X and A electronic states are A_1 and A_2 at the Franck–Condon point of C_{2v} symmetry.

The transition amplitudes between field-dressed states $|\Phi_k(n)\rangle$ and $|\Phi_l(n)\rangle$ within the framework of first-order time-dependent perturbation theory can be obtained as

$$\langle\Phi_k(n)|\hat{d}_\alpha|\Phi_l(n)\rangle = \sum_{ij} C_{\mathrm{X}i}^{(k)*} C_{\mathrm{X}j}^{(l)} \langle \mathrm{X}i|\hat{d}_\alpha|\mathrm{X}j\rangle + \sum_{ij} C_{\mathrm{A}i}^{(k)*} C_{\mathrm{A}j}^{(l)} \langle \mathrm{A}i|\hat{d}_\alpha|\mathrm{A}j\rangle \tag{3}$$

where $\hat{d}_\alpha$ is the electric dipole moment operator ($\alpha = x, y, z$). One can notice that the transitions $|\Phi_k(n)\rangle \rightarrow |\Phi_l(n)\rangle$ are associated with the PDM related to the electronic states X and A. The corresponding transition angular frequencies and intensities are $\omega_{kl} = (\epsilon_l(n) - \epsilon_k(n))/\hbar$ and $I_{kl} \propto \omega_{kl} \sum_\alpha |\langle\Phi_k(n)|\hat{d}_\alpha|\Phi_l(n)\rangle|^2$, respectively. Equation 3 serves as our working formula for the computation of the low-energy part of the vibronic spectrum and for the interpretation of the peaks appearing below 1100 cm^{-1} in the field-dressed spectrum of Figure 1. For further discussion of the spectroscopy of field-dressed molecules we refer to ref. 41.

The dressing situation corresponding to the field-dressed spectrum in Figure 1 is featured in Figure 2 where one-dimensional cuts of the V_{X} and V_{A} PESs are shown along the ν_2 (C=O stretch) normal mode (normal coordinates other than Q_2 are set to zero). In Figure 2, the system is dressed with photons corresponding to $\omega = 32932.5$ cm^{-1} and the V_{A} PES is shifted down with the energy of the dressing photon, see eq 1. Consequently, the vibrational ground state of X becomes nearly resonant with multiple close-lying excited vibrational eigenstates of

A and the resulting field-dressed states can be described as superpositions of the eigenstates mentioned. Figure 3 provides two-dimensional cuts of the light-induced adiabatic PESs. The two-dimensional cuts, given as functions of the Q_2 (C=O stretch) and Q_4 (out-of-plane bend) normal coordinates (the remaining four normal coordinates are set to zero), clearly show that a LICI is formed between the two light-induced adiabatic PESs.

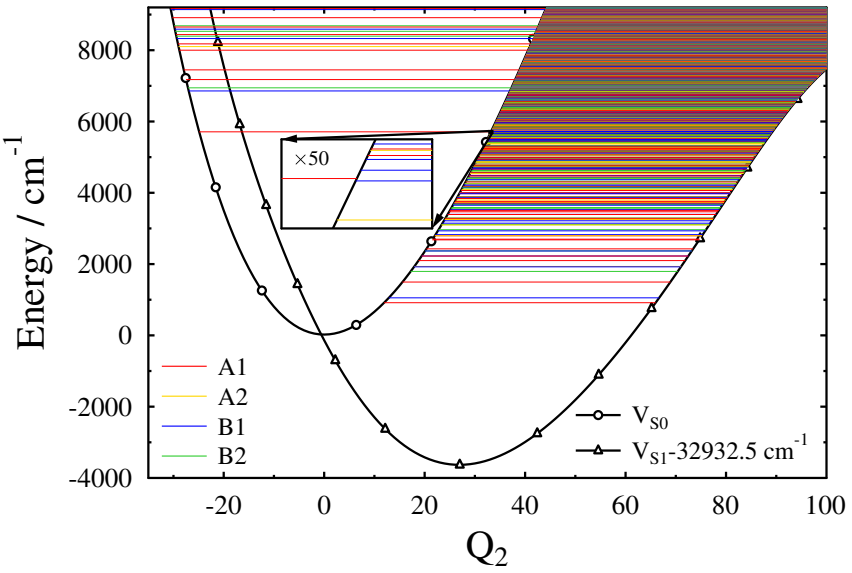

Figure 2: One-dimensional field-free potential energy cuts along the ν_2 (C=O stretch) normal mode. The excited-state potential curve (V_{S1} in the figure) is shifted down by the photon energy value corresponding to 32932.5 cm^{-1} (see eq 1). Vibrational energy levels are indicated by horizontal lines with colors encoding irreducible representations of the C_{2v} point group. Due to the high density of S_1 states in six degrees of freedom, levels of S_1 become quasi-degenerate with levels of S_0 and interact with them non-adiabatically.

Having discussed the underlying theory and dressing mechanism, we can finally move on to the detailed analysis of the field-dressed spectrum in Figure 1. In what follows we assume that the dressing field is switched on adiabatically and the initial field-dressed state $|\Phi_i(n)\rangle$ is chosen as the field-dressed state which gives maximal overlap with the vibrational ground state of the X electronic state. The newly-emerging peaks, readily visible in the lower panel of Figure 1, can be classified into four main groups. The first two groups consist of peaks between $400-650$ cm^{-1} (g_1) and $700-800$ cm^{-1} (g_2), while the third and fourth groups involve peaks located in the intervals $800-900$ cm^{-1} (g_3) and $1000-1100$ cm^{-1} (g_4). The

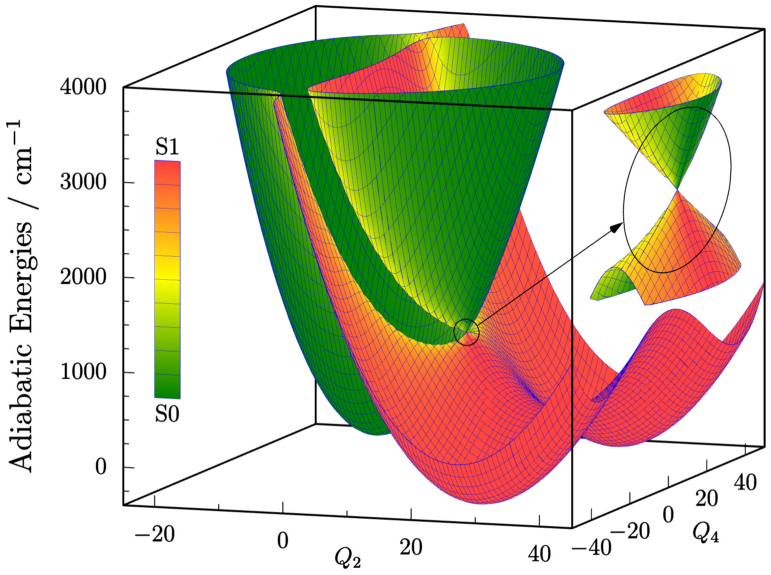

Figure 3: Two-dimensional light-induced adiabatic potential energy surfaces along the ν_2 (C=O stretch) and ν_4 (out-of-plane bend) normal modes. The dressing wavenumber and intensity are chosen as $\omega_\mathrm{d} = 29000$ cm^{-1} and $I_\mathrm{d} = 10^{14}$ W/cm^2, respectively, and the dressing field is polarized along the body-fixed y axis. These dressing wavenumber and intensity values are chosen for a better visualization only. The light-induced conical intersection is highlighted in the inset on the right-hand side of the figure. The character of the adiabatic potential energy surfaces is indicated by different colors (see the legend on the left).

transitions of g_1 and g_2 types are all polarized along the body-fixed x axis, while the g_3 and g_4 transitions are polarized along the body-fixed y (hardly discernible in Figure 1) and z axes, respectively.

The peaks appearing below 1100 cm^{-1} in the field-dressed spectrum can be attributed to admixtures of the vibrational eigenstates of the A electronic state in the initial field-dressed state $|\Phi_\mathrm{i}(n)\rangle$. $|\Phi_i(n)\rangle$ in this particular case is a superposition of the X vibrational ground state (0.0 cm^{-1}, A_1 symmetry, 52.3%) and two close-lying A vibrational eigenstates of B_1 symmetry, namely 32931.2 cm^{-1} (36.0%) and 32937.2 cm^{-1} (11.5%) where the numbers in the parentheses indicate the populations of the vibrational eigenstates in $|\Phi_\mathrm{i}(n)\rangle$. Note that the inset in Figure 2 shows the two close-lying A vibrational eigenstates mentioned (two lowest blue lines on the right) that are coupled to the X vibrational ground state (red line on the left) by the dressing field. As the dressing field is polarized along the body-fixed y axis and the body-fixed y component of the TDM transforms according to the B_1 irreducible

representation (see Table S3 in the Supporting Information), the X vibrational ground state (A_1 symmetry) can be coupled only to vibrational eigenstates of B_1 symmetry of the A electronic state by the dressing field.

A detailed analysis of the field-dressed states has revealed that the final field-dressed state $|\Phi_f(n)\rangle$ for each peak below 1100 cm^{-1} remains an eigenstate of the field-free molecule and has the form $|\Phi_f(n)\rangle = |Aj\rangle|n-1\rangle$ to a good approximation. Therefore, the peaks below 1100 cm^{-1} can be interpreted as transitions from the vibrational eigenstates of A at 32931.2 cm^{-1} and 32937.2 cm^{-1} (both of B_1 symmetry) to other A vibrational eigenstates making up the final field-dressed states and they are associated with the PDM of the A electronic state according to the second term in eq 3. The richness of the field-dressed spectrum can be primarily attributed to the ν_4 mode as the anharmonic double-well nature of the V_A PES along the ν_4 mode can lead to multiple changes in the vibrational quantum number v_4 ($|\Delta v_4| = 0, 1, 2, 3, \dots$). The emergence of peaks in the interval $0 - 1100$ cm^{-1} can be interpreted as intensity borrowing whereby the intensity is borrowed from peaks that are also present in the field-free vibrational spectrum.

Similar intensity borrowing effects are observed for many other laser parameters. Figure 4, for instance, compares the field-free and field-dressed spectra for a different laser frequency, $\omega_d = 34189.5$ cm^{-1} ($\lambda_d = 292.49$ nm). Similarly to Figure 1, several peaks below 1100 cm^{-1} appear in the field-dressed spectrum, which can again be understood by the aforementioned mechanism.

In the present work we have outlined a pump-probe scheme to obtain the field-dressed low-energy vibronic spectra of polyatomic molecules treating all vibrational degrees of freedom. The H_2CO molecule which does not exhibit a natural conical intersection in the studied energy region was chosen as a showcase example. In order to calculate the weak-field absorption and stimulated emission spectra of the field-dressed H_2CO molecule we performed accurate, six-dimensional computations with different dressing photon energies and dressing field intensities.

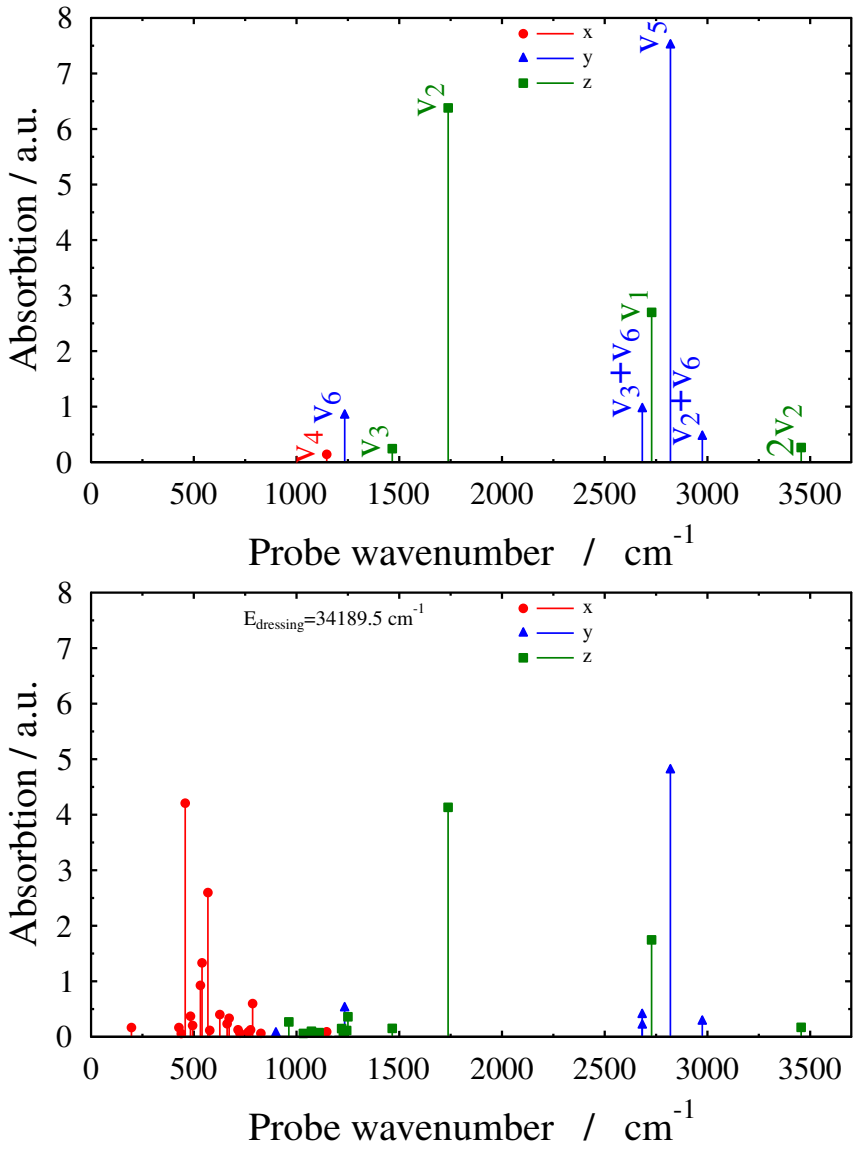

Figure 4: Impact of light-induced non-adiabaticity on the vibrational spectrum of H_2CO for a somewhat higher laser frequency than that used in Figure 1. Upper panel: field-free vibrational spectrum. Lower panel: spectrum in the laser field. The dressing frequency is $\omega_d = 34189.5\ \mathrm{cm}^{-1}$. All other details are as in Figure 1. The figure shows that the prominent appearance of low-lying light-induced levels is not unique, but the details depend sensitively on the laser parameters.

The results obtained clearly show the direct impact of the light-induced conical intersection on the field-dressed spectra of the H_2CO molecule. The findings are highly sensitive to variations of the dressing frequency which varies the location of the LICI, shedding light on the mixing of the levels of different electronic states and on their coupling mechanism. The emergence of peaks in the field-dressed spectrum below 1100 cm^{-1} undoubtedly demonstrates strong nonadiabatic effects manifested in the so-called "intensity borrowing" phenomenon, arising due to the presence of the light-induced nonadiabaticity. The strong nonadiabaticity which is completely absent in the field-free H_2CO molecule mixes the different electronic and vibrational degrees of freedom creating a very rich pattern in a certain interval of the low-energy vibronic spectrum where no transitions occur in the field-free situation. This intense mixing process could not happen without the presence of the light-induced conical intersection. The clear-cut intensity borrowing mechanism discussed here is general and not restricted to H_2CO. It can be expected to be generically operative in polyatomics. The more degrees of freedom the molecule has, the higher the vibrational level density is and the more borrowing effects one can expect.

Acknowledgement

Professor Joel Bowman is gratefully acknowledged for providing Fortran subroutines for the S_0 and S_1 potential energy surfaces. This research was supported by the EU-funded Hungarian grant EFOP-3.6.2-16-2017-00005. The authors are grateful to NKFIH for financial support (grants No. K128396 and PD124699).

Supporting Information Available

Equilibrium structure and normal modes of the H_2CO molecule, technical details of the computations. This material is available free of charge via the Internet at `http://pubs.acs.org/`.

References

(1) Köppel, H.; Domcke, W.; Cederbaum, L. S. Multimode Molecular Dynamics Beyond the Born–Oppenheimer Approximation. *Adv. Chem. Phys.* **1984**, *57*, 59–246.

(2) Yarkony, D. R. Diabolical conical intersections. *Rev. Mod. Phys.* **1996**, *68*, 985–1013.

(3) Baer, M. Introduction to the theory of electronic non-adiabatic coupling terms in molecular systems. *Phys. Rep.* **2002**, *358*, 75 – 142.

(4) Worth, G. A.; Cederbaum, L. S. Beyond Born–Oppenheimer: Molecular Dynamics Through a Conical Intersection. *Ann. Rev. Phys. Chem.* **2004**, *55*, 127–158.

(5) Domcke, W.; Yarkony, D. R.; Köppel, H. *Conical Intersections*; World Scientific, 2004.

(6) Baer, M. *Beyond Born–Oppenheimer: Electronic Non-Adiabatic Coupling Terms and Conical Intersections*; Wiley, New York, 2006.

(7) Lim, J. S.; Kim, S. K. Experimental probing of conical intersection dynamics in the photodissociation of thioanisole. *Nat. Chem.* **2010**, *2*, 627–632.

(8) Wörner, H. J.; Bertrand, J. B.; Fabre, B.; Higuet, J.; Ruf, H.; Dubrouil, A.; Patchkovskii, S.; Spanner, M.; Mairesse, Y.; Blanchet, V. et al. Conical Intersection Dynamics in NO_2 Probed by Homodyne High-Harmonic Spectroscopy. *Science* **2011**, *334*, 208–212.

(9) You, H. S.; Han, S.; Lim, J. S.; Kim, S. K. ($\pi\pi^*/\pi\sigma^*$) Conical Intersection Seam Experimentally Observed in the S-D Bond Dissociation Reaction of Thiophenol-d_1. *J. Phys. Chem. Lett.* **2015**, *6*, 3202–3208.

(10) Musser, A. J.; Liebel, M.; Schnedermann, C.; Wende, T.; Kehoe, T. B.; Rao, A.; Kukura, P. Evidence for conical intersection dynamics mediating ultrafast singlet exciton fission. *Nat. Phys.* **2015**, *11*, 352–357.

(11) von Conta, A.; Tehlar, A.; Schletter, A.; Arasaki, Y.; Takatsuka, K.; Wörner, H. J. Conical-intersection dynamics and ground-state chemistry probed by extreme-ultraviolet time-resolved photoelectron spectroscopy. *Nat. Commun.* **2018**, *9*, 3162.

(12) Corrales, M. E.; González-Vázquez, J.; de Nalda, R.; Bañares, L. Coulomb Explosion Imaging for the Visualization of a Conical Intersection. *J. Phys. Chem. Lett.* **2019**, *10*, 138–143.

(13) Martinez, T. J. Seaming is believing. *Nature* **2010**, *467*, 412–413.

(14) Kowalewski, M.; Bennett, K.; Dorfman, K. E.; Mukamel, S. Catching Conical Intersections in the Act: Monitoring Transient Electronic Coherences by Attosecond Stimulated X-Ray Raman Signals. *Phys. Rev. Lett.* **2015**, *115*, 193003.

(15) Xie, C.; Ma, J.; Zhu, X.; Yarkony, D. R.; Xie, D.; Guo, H. Nonadiabatic Tunneling in Photodissociation of Phenol. *J. Am. Chem. Soc.* **2016**, *138*, 7828–7831.

(16) DeVine, J. A.; Weichman, M. L.; Zhou, X.; Ma, J.; Jiang, B.; Guo, H.; Neumark, D. M. Non-Adiabatic Effects on Excited States of Vinylidene Observed with Slow Photoelectron Velocity-Map Imaging. *J. Am. Chem. Soc.* **2016**, *138*, 16417–16425.

(17) Woo, K. C.; Kang, D. H.; Kim, S. K. Real-Time Observation of Nonadiabatic Bifurcation Dynamics at a Conical Intersection. *J. Am. Chem. Soc.* **2017**, *139*, 17152–17158.

(18) Curchod, B. F. E.; Martínez, T. J. Ab Initio Nonadiabatic Quantum Molecular Dynamics. *Chem. Rev.* **2018**, *118*, 3305–3336.

(19) Bennett, K.; Kowalewski, M.; Rouxel, J. R.; Mukamel, S. Monitoring molecular nonadiabatic dynamics with femtosecond X-ray diffraction. *Proc. Natl. Acad. Sci. U.S.A.* **2018**, *115*, 6538–6547.

(20) Ryabinkin, I. G.; Joubert-Doriol, L.; Izmaylov, A. F. Geometric Phase Effects in Nonadiabatic Dynamics near Conical Intersections. *Acc. Chem. Res.* **2017**, *50*, 1785–1793.

(21) Xie, C.; Malbon, C. L.; Guo, H.; Yarkony, D. R. Up to a Sign. The Insidious Effects of Energetically Inaccessible Conical Intersections on Unimolecular Reactions. *Acc. Chem. Res.* **2019**, *52*, 501–509.

(22) Born, M.; Oppenheimer, R. Zur Quantentheorie der Molekeln. *Ann. Phys.* **1927**, *389*, 457–484.

(23) von Neumann, J.; Wigner, E. P. Über das Verhalten von Eigenwerten bei adiabatischen Prozessen. *Z. Physik* **1929**, *30*, 467–470.

(24) Coe, J. D.; Martínez, T. J. Competitive Decay at Two- and Three-State Conical Intersections in Excited-State Intramolecular Proton Transfer. *J. Am. Chem. Soc.* **2005**, *127*, 4560–4561.

(25) Boggio-Pasqua, M.; Groenhof, G.; Schäfer, L. V.; Grubmüller, H.; Robb, M. A. Ultrafast Deactivation Channel for Thymine Dimerization. *J. Am. Chem. Soc.* **2007**, *129*, 10996–10997.

(26) Matsika, S.; Yarkony, D. R. Conical Intersections of Three Electronic States Affect the Ground State of Radical Species with Little or No Symmetry: Pyrazolyl. *J. Am. Chem. Soc.* **2003**, *125*, 12428–12429.

(27) Xie, C.; Malbon, C. L.; Yarkony, D. R.; Xie, D.; Guo, H. Signatures of a Conical Intersection in Adiabatic Dissociation on the Ground Electronic State. *J. Am. Chem. Soc.* **2018**, *140*, 1986–1989.

(28) Moiseyev, N.; Šindelka, M.; Cederbaum, L. S. Laser-induced conical intersections in molecular optical lattices. *J. Phys. B: At. Mol. Opt. Phys.* **2008**, *41*, 221001.

(29) Šindelka, M.; Moiseyev, N.; Cederbaum, L. S. Strong impact of light-induced conical intersections on the spectrum of diatomic molecules. *J. Phys. B: At. Mol. Opt. Phys.* **2011**, *44*, 045603.

(30) Halász, G. J.; Vibók, Á.; Šindelka, M.; Moiseyev, N.; Cederbaum, L. S. Conical intersections induced by light: Berry phase and wavepacket dynamics. *J. Phys. B: At. Mol. Opt. Phys.* **2011**, *44*, 175102.

(31) Halász, G. J.; Šindelka, M.; Moiseyev, N.; Cederbaum, L. S.; Vibók, A. Light-Induced Conical Intersections: Topological Phase, Wave Packet Dynamics, and Molecular Alignment. *J. Phys. Chem. A* **2012**, *116*, 2636–2643.

(32) Halász, G. J.; Vibók, A.; Moiseyev, N.; Cederbaum, L. S. Nuclear-wave-packet quantum interference in the intense laser dissociation of the D_2^+ molecule. *Phys. Rev. A* **2013**, *88*, 043413.

(33) Halász, G. J.; Badankó, P.; Vibók, A. Geometric phase of light-induced conical intersections: adiabatic time-dependent approach. *Mol. Phys.* **2018**, *116*, 2652–2659.

(34) Natan, A.; Ware, M. R.; Prabhudesai, V. S.; Lev, U.; Bruner, B. D.; Heber, O.; Bucksbaum, P. H. Observation of Quantum Interferences via Light-Induced Conical Intersections in Diatomic Molecules. *Phys. Rev. Lett.* **2016**, *116*, 143004.

(35) Halász, G. J.; Vibók, A.; Cederbaum, L. S. Direct Signature of Light-Induced Conical Intersections in Diatomics. *J. Phys. Chem. Lett.* **2015**, *6*, 348–354.

(36) Csehi, A.; Halász, G. J.; Cederbaum, L. S.; Vibók, A. Towards controlling the dissociation probability by light-induced conical intersections. *Faraday Discuss.* **2016**, *194*, 479–493.

(37) Csehi, A.; Halász, G. J.; Cederbaum, L. S.; Vibók, A. Intrinsic and light-induced nonadiabatic phenomena in the NaI molecule. *Phys. Chem. Chem. Phys.* **2017**, *19*, 19656–19664.

(38) Csehi, A.; Halász, G. J.; Cederbaum, L. S.; Vibók, A. *Attosecond Molecular Dynamics*; The Royal Society of Chemistry, 2018; pp 183–217.

(39) Szidarovszky, T.; Halász, G. J.; Császár, A. G.; Cederbaum, L. S.; Vibók, A. Direct Signatures of Light-Induced Conical Intersections on the Field-Dressed Spectrum of Na_2. *J. Phys. Chem. Lett.* **2018**, *9*, 2739–2745.

(40) Szidarovszky, T.; Halász, G. J.; Császár, A. G.; Cederbaum, L. S.; Vibók, A. Conical Intersections Induced by Quantum Light: Field-Dressed Spectra from the Weak to the Ultrastrong Coupling Regimes. *J. Phys. Chem. Lett.* **2018**, *9*, 6215–6223.

(41) Szidarovszky, T.; Császár, A. G.; Halász, G. J.; Vibók, A. Rovibronic spectra of molecules dressed by light fields. *Phys. Rev. A* **2019**, *100*, 033414.

(42) Pawlak, M.; Szidarovszky, T.; Halász, G. J.; Vibók, A. Robust field-dressed spectra of diatomics in an optical lattice. *Phys. Chem. Chem. Phys.* **2020**, *22*, 3715–3723.

(43) Kim, J.; Tao, H.; White, J. L.; Petrović, V. S.; Martinez, T. J.; Bucksbaum, P. H. Control of 1,3-Cyclohexadiene Photoisomerization Using Light-Induced Conical Intersections. *J. Phys. Chem. A* **2012**, *116*, 2758–2763.

(44) Corrales, M. E.; González-Vázquez, J.; Balerdi, G.; Solá, I. R.; de Nalda, R.; Bañares, L. Control of ultrafast molecular photodissociation by laser-field-induced potentials. *Nat. Chem.* **2014**, *6*, 785–790.

(45) Demekhin, P. V.; Cederbaum, L. S. Light-induced conical intersections in polyatomic molecules: General theory, strategies of exploitation, and application. *J. Chem. Phys.* **2013**, *139*, 154314.

(46) Araujo, M.; Lasorne, B.; Bearpark, M. J.; Robb, M. A. The Photochemistry of Formaldehyde: Internal Conversion and Molecular Dissociation in a Single Step? *J. Phys. Chem. A* **2008**, *112*, 7489–7491.

(47) Araújo, M.; Lasorne, B.; Magalhães, A. L.; Worth, G. A.; Bearpark, M. J.; Robb, M. A. The molecular dissociation of formaldehyde at medium photoexcitation energies: A

quantum chemistry and direct quantum dynamics study. *J. Chem. Phys.* **2009**, *131*, 144301.

(48) Araújo, M.; Lasorne, B.; Magalhães, A. L.; Bearpark, M. J.; Robb, M. A. Controlling Product Selection in the Photodissociation of Formaldehyde: Direct Quantum Dynamics from the S_1 Barrier. *J. Phys. Chem. A* **2010**, *114*, 12016–12020.

(49) Chu, S. Floquet theory and complex quasivibrational energy formalism for intense field molecular photodissociation. *J. Chem. Phys.* **1981**, *75*, 2215–2221.

(50) Chu, S.-I.; Telnov, D. A. Beyond the Floquet theorem: generalized Floquet formalisms and quasienergy methods for atomic and molecular multiphoton processes in intense laser fields. *Phys. Rep.* **2004**, *390*, 1 – 131.

(51) Mátyus, E.; Czakó, G.; Császár, A. G. Toward Black-Box-Type Full- and Reduced-Dimensional Variational (Ro)vibrational Computations. *J. Chem. Phys.* **2009**, *130*, 134112.

(52) Fábri, C.; Mátyus, E.; Császár, A. G. Rotating full- and reduced-dimensional quantum chemical models of molecules. *J. Chem. Phys.* **2011**, *134*, 074105.

(53) Császár, A. G.; Fábri, C.; Szidarovszky, T.; Mátyus, E.; Furtenbacher, T.; Czakó, G. The Fourth Age of Quantum Chemistry: Molecules in Motion. *Phys. Chem. Chem. Phys.* **2012**, *14*, 1085–1106.

(54) Wang, X.; Houston, P. L.; Bowman, J. M. A new (multi-reference configuration interaction) potential energy surface for H_2CO and preliminary studies of roaming. *Philos. Trans. R. Soc. A* **2017**, *375*, 20160194.

(55) Fu, B.; Shepler, B. C.; Bowman, J. M. Three-State Trajectory Surface Hopping Studies of the Photodissociation Dynamics of Formaldehyde on ab Initio Potential Energy Surfaces. *J. Am. Chem. Soc.* **2011**, *133*, 7957–7968.